Jurnal Teknologi Reaktor Nuklir

Tri Dasa Mega

Journal homepage: htpps://ejurnal.brin.go.id/tridam

Dose Analysis of Prostate Cancer Therapy with X-Ray Therapy using PHITS Program Version 3.341

Tri Nanda Febriansyah[1*], Beta Nur Pratiwi[1], Subur Pramono[1], Yohannes Sardjono[2], Isman Mulyadi Triatmoko[2], Gede Sutresna Wijaya[2], Heru Prasetio[2], Nur Rahmah Hidayati[2], Nunung Nuraeni[2], Syarifatul Ulya[2], Zuhdi Ismail[2]

[1] *Department of Physics, Faculty of Science, Sultan Maulana Hasanuddin State Islamic University, 42171, Banten, Indonesia*

[2] *Research Center for Safety, Metrology and Nuclear Quality Technology, Research Organization for Nuclear Energy, The National Research and Innovation Agency, Tangerang Selatan, Indonesia*

ARTICLE INFO

Article history:
Received: Dec 03, 2024
Received in revised form: Jan 15, 2025
Accepted: Jan 20, 2025

Keywords:

Prostate Cancer
Dosimetry
Radiotherapy
X-Ray Therapy
PHITS V. 3. 341

A B S T R A C T

According to statistics from the WHO, in 2022, prostate cancer was ranked 4th out of 15 cancers that cause the highest deaths in the world. Prostate cancer forms in the prostate gland cells. Most prostate cancers are slow-growing and unlikely to spread, but some can grow faster. The position and dimensions of prostate cancer are visualized with MRI so that treatment methods can be performed with X-ray therapy through LINAC. This study used PHITS to simulate X-ray therapy using a voxel or phantom model. The phantom used was based on an American adult male from the ORNL Phantom. The treatment was simulated using three irradiation directions of 0°, 45°, and 90°. The results stated that 33-35 fractions were required to achieve a total 65-70 Gy dose. The more optimal irradiation direction is at 45 degrees, with 1.66 Gy per fraction on the skin and 1.99 Gy per fraction on cancer cells, with a total absorbed dose of 65.8-69.8 Gy.

1. INTRODUCTION

Cancer represents a major challenge to society, public health, and the economy in the 21st century. It accounts for nearly one in six deaths (16.8%) and a quarter (22.8%) of non-communicable disease (NCD) fatalities worldwide. Prostate cancer is responsible for 30.3% of premature deaths caused by non-communicable diseases (NCDs) in individuals aged 30 - 69, making it one of the top three causes of death for this age group across 177 countries. Lung cancer is the most diagnosed cancer worldwide, accounting for 12.4% of total cases, followed by breast cancer in women at 11.6%, colorectal cancer at 9.6%, prostate cancer at 7.3%, and stomach cancer at 4.9%. Prostate cancer is the most frequently diagnosed cancer in men across 118 countries [1]. Prostate cancer forms in the prostate gland cells. Most prostate cancers are slow-growing and unlikely to spread, but some can grow faster [2]. Prostate cancer is the fifth most common cancer among men in Indonesia, with 13,130 cases reported in 2022.

Radiotherapy is frequently used in cancer treatment, either alone or combined with other conventional methods such as surgery, chemotherapy, and immunotherapy [4]. Radiotherapy contributes significantly to the treatment of prostate cancer [5]. One type of radiotherapy is external radiotherapy, which is performed by firing particles directed at the body, such as protons, neutrons, X-rays, or gamma rays [6]. X-rays are generated when the kinetic energy of electrons accelerated by an

* Corresponding Author:
Email:trinandafebriansyah03@gmail.com
DOI:10.55981/tdm.2025.7158

electric field from a specific voltage (measured in volts, *V*), which is then converted into electromagnetic radiation through collisions and radiation interactions [7]. Medical facilities need a systematic cancer patient dose management system and a national infrastructure [8].

Linear accelerators (LINACs) are devices commonly used in external radiation therapy for cancer treatment [9]. In a LINAC, electrons are accelerated to near the speed of light. These high-energy electrons produce X-rays when colliding with a heavy metal target [10]. At the atomic level, ionizing radiation works by ionizing atoms, i.e., releasing electrons from their orbits. While at the cellular level, the main impact of radiation is DNA damage [11]. MRI is a frequently used tool to support the diagnosis of cancer cells.

Magnetic resonance imaging (MRI) is an advanced diagnostic tool used to examine and detect body conditions using strong magnetic fields and radio frequency waves. This method does not use X-rays or radioactive materials, making it very safe for many people. MRI produces images that can show differences very clearly and are more sensitive in assessing soft tissue anatomy in the body compared to examinations using X-rays or CT scans [12]. MRI facilitates the identification of Organs at Risk (OAR) around critical areas near the target boundary [13], such as adjacent normal tissues, such as the rectum, pelvic bones, bladder, colon, small intestine, femoral head, and others [14].

The Particle and Heavy Ion Transport Code System (PHITS) is a Monte Carlo-based radiation transport code that simulates particle behavior, with energies up to 1 TeV per nucleon for ions [15], meanwhile, other software such as MCNPX has a maximum energy limit for photon transport set at 100 GeV, while for electron transport it is 1 GeV [16]. PHITS can calculate doses for various types of radiation. Therefore, PHITS can also simulate X-ray therapy using voxel or phantom models [17]. The selection of ionizing radiation dosimeters is essential, especially for low exposures, and should not be overlooked [18]. The total dose should be around 65-70 Gy, with 25-28 times fraction administration. This makes it an alternative treatment option to prostate radiotherapy with standard fractional methods [14]. Previous studies related to the use of X-ray therapy for prostate cancer therapy are the primary reference in determining parameters and predicting the results of this study.

2. RESEARCH METHOD

2.1. Simulating the linear geometry of accelerators

This research was conducted with the Particle and Heavy Ions Transport Code System (PHITS) simulation program version 3.341 licensed by JAEA. The model geometry was developed with Notepad++, while the output of the PHITS code was then processed with Microsoft Excel 2016. All simulations were carried out with a 1.50 GHz processor up to 8 threads with 16 GB RAM.

The reference phantom voxel being modeled with PHITS came from the ORNL phantom for an American adult male. In addition, the system used for X-ray therapy simulation was the ELEKTA Precise Linac, with a specific model of Versa HD [19]. In this study, a model of a 10 MV linear accelerator (LINAC) has been developed for simulations, as shown in Fig. 1. This accelerator requires that the beam current at 10 MeV must be at least 1.8 mA [20]. The parameters used in the simulation of LINAC-based X-ray therapy are presented in Table 1.

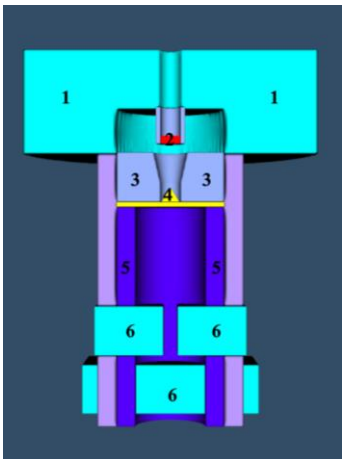

Figure 1. Elekta Versa HD LINAC Head Geometry Design, with description (1) Outer shielding, (2) Target (tungsten), (3) Primary collimator, (4) Flattening filter, (5) Inner shielding, (6) Secondary collimator (JAWS)

Table 1. Specification of Simulated X-ray Therapy for Prostate Cancer

No	Parameters	Description
1.	Beam energy [20]	10 MeV
2.	Particle [19]	Electron
3.	Beam intensity [19]	0.6653
4.	Normalization factor [20]	1.12×10^{15}
5.	Size of beam	0.5 cm (radius)
6.	Irradiance angle variation [21]	$0°, 45°, 90°$
7.	SSD [22]	80 cm
8.	Particle count in the simulation	100.000
9.	Total batches in the simulation	50

2.2. Creating a simulation of the patient's body and its organs

Analyzing the dose distribution in cancer therapy is crucial to ensure that the dose is precisely absorbed by the target tumor while minimizing exposure to surrounding healthy tissue. The simulation software employed for this purpose is PHITS with its Monte Carlo (MC) method to optimize the x-ray direction and dose to tumor cells.

Essentially, MC methods involve generating a large set of potential values for the parameter of interest and substituting integration with a sample mean. In practice, these parameter values can be derived by physically replicating the relevant experiment or by probabilistically characterizing it to produce a series of random outcomes [23].

Phantoms have been created using various materials that mimic body tissues to simulate the radiation transport process in the human body [24]. In this study, an American adult male ORNL phantom was used. Cancer is characterized by a yellow line as Gross Tumor Volume (GTV) shown in Figure 2. Clinical Target Volume (CTV) includes the entire prostate gland, including the prostate capsule, as well as macroscopic disease outside the capsule, with an additional 3 mm expansion in 3D [26].

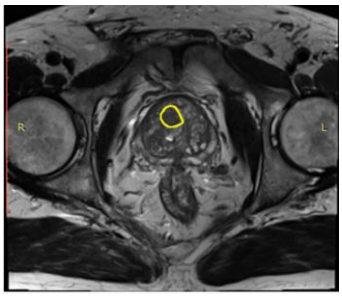

Figure 2. MRI imaging of prostate cancer with cancer size 1.8 × 1.8 × 3.5 mm [25]

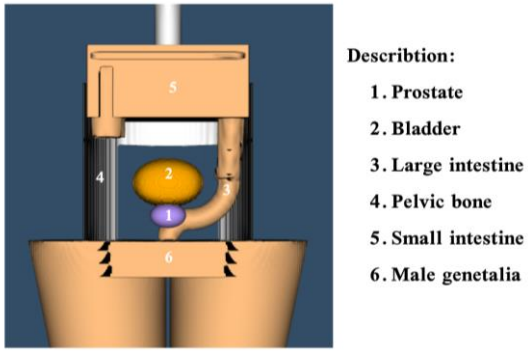

Figure 3. Prostate cancer OAR voxel geometry

Prostate cancer frequently manifests as multiple foci and impacts both lobes. Consequently, the Clinical Target Volume (CTV) should encompass the entire prostate and its capsule [14]. Typically, the Planning Target Volume (PTV) is defined as a 0.5 cm margin surrounding the Clinical Target Volume (CTV) [27]. Organs at risk (OARs) around the critical area near the target boundary OARs of the prostate, rectum, small intestine, bladder, colon, pelvic bone, and others, as shown in Figure 3, with the focus on the cancerous part seen in Figure 4.

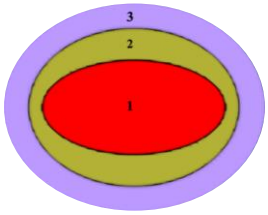

Figure 4. Prostate cancer tissue geometry

2.3. Dose distribution

Through the current Linear Accelerator, a normalization factor is obtained to determine the dose rate shown in equation (1)

$$Normalization\ factor = \frac{I\ [\mathrm{C/s}] \times T\ [\mathrm{s}] \times F}{charge\ per\ unit\ particle} \quad (1)$$

with I as current (A), T as time (s), and F as a duty factor, the normalization factor is used as a multiplying factor in the tally deposit parameter, to obtain the particle distribution [28],[29].

The irradiation time is determined by dividing the minimum dose capable of harming cancerous tissue by the dose rate, as indicated in (2) [30]. The minimum dose that damages cancer tissue used was 65 Gy.

$$irradiation\ time\ (s) = \frac{minimum\ dose\ of\ damage\ in\ cancer\ (Gy)}{total\ dose\ rate\ (Gy\ /\ s)} \quad (2)$$

The absorbed dose refers to the quantity of radiation energy taken in by tissues or organs in the human body [31]. The absorbed dose is given by (3) [30]:

$$Absorption\ dose(Gy) = Dose\ Rate\left(\frac{Gy}{s}\right) \times irradiation\ time(s) \quad (3)$$

The SI unit for absorbed dose is joules per kilogram (J/kg), called Grays (Gy).

The equivalent dose (H_T) is determined by multiplying the absorbed dose ($D_{T,R}$) by the radiation weighting factor (w_R), which indicates the relative effectiveness of the radiation type in inducing biological damage. This is expressed as (4).

$$H_T = \sum_R w_R D_{T,R} \quad (4)$$

Here, $D_{T,R}$ represents the average absorbed dose to organ or tissue T from the radiation of the type R, while w_R denotes the radiation weighting factor. The factor w_R is utilized to compute the dose equivalent of the average absorbed dose to a tissue or organ. For X-ray radiation, the weighting factor is w_R =1. The unit for equivalent dose is joules per kilogram (J/kg), commonly referred to as Sievert (Sv) [31].

The effective dose (E) is the weighted sum of the equivalent doses in all organs and tissues of the body, as expressed in (5).

$$E = \sum_T w_T H_T \qquad (5)$$

In this context, $\boldsymbol{E}$ represents the effective dose, and $\boldsymbol{w_T}$ is the tissue weighting factor. The tissue weighting factor ($\boldsymbol{w_T}$) indicates the relative contribution of that organ or tissue to the overall radiation effects on human health due to stochastic outcomes [31].

3. RESULTS AND DISCUSSION

The simulated prostate cancer therapy results demonstrate a particle distribution that aligns with the intended target volume, as illustrated in Figure 5. This distribution suggests that the radiation dose effectively concentrates on the tumor region while minimizing exposure to adjacent healthy tissue.

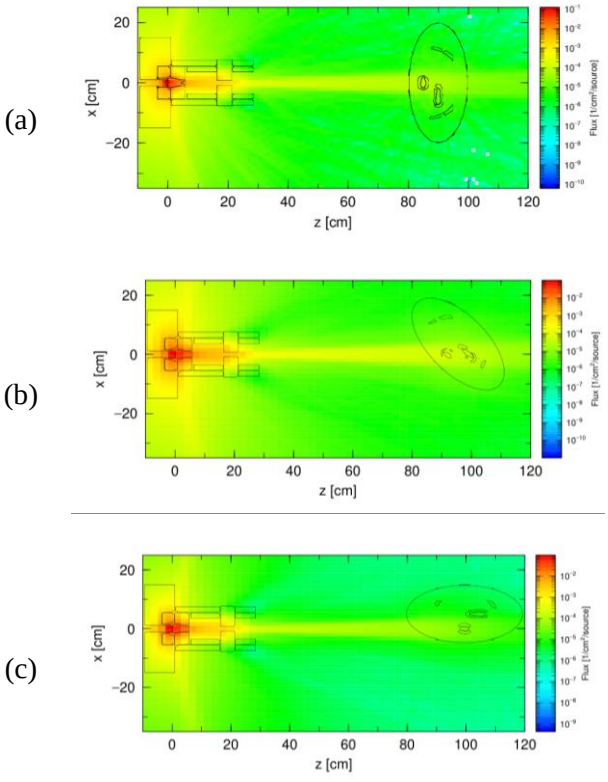

Fig. 5. Particle Distribution Simulation, (a) 0-degree irradiation direction, (b) 45-degree irradiation direction, (c) 90-degree irradiation direction (with x = width and z = depth)

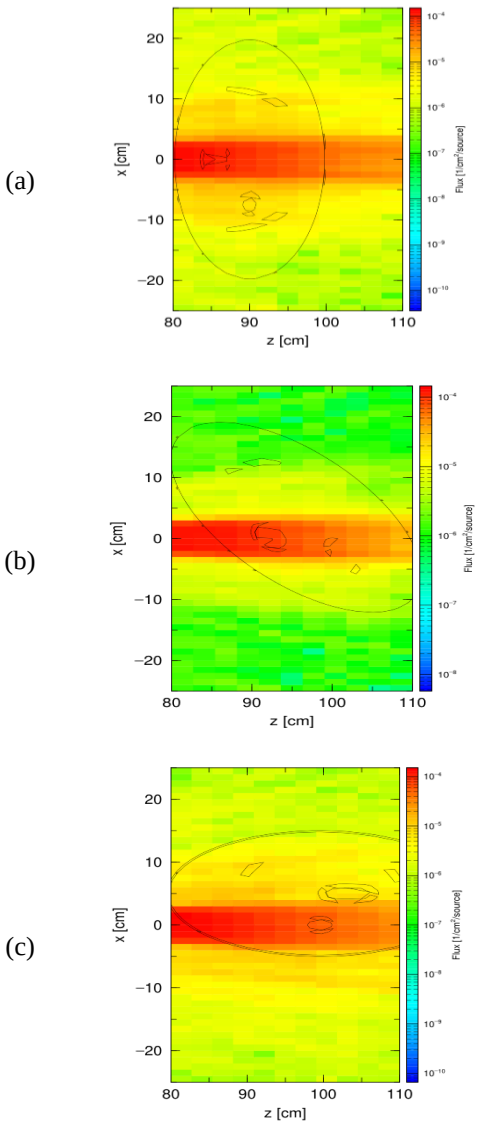

Figure 6. Focused particle distribution on cancer cells, (a) 0-degree irradiation direction, (b) 45-degree irradiation direction, (c) 90-degree irradiation direction (with x = width and z = depth)

From equation (2), irradiation time can be obtained as shown in Table 3, which also shows that the variation of irradiation direction affects irradiation time and beam-on time. The time duration varies according to the change in irradiation direction at angles of 0°, 45°, and 90°.

Table 2. Dose rate data with variations in irradiation direction

Direction of Illumination	Organ	Dose Rate (Gy/s)
0°	Skin	0.024742
	Prostate	0.028068
	GTV	0.028068
	CTV	0.028068
	PTV	0.028068
45°	Skin	0.021944
	Prostate	0.026413
	GTV	0.026413
	CTV	0.026413
	PTV	0.026413
90°	Skin	0.024143
	Prostate	0.022771
	GTV	0.022771
	CTV	0.022771
	PTV	0.022771

Table 3. Irradiation time data

Direction of Illumination	Irradiation time		Beam-on Time	
	sec	minutes	sec	minutes
0°	2316	38.6	71.0	1.18
45°	2461	41.0	75.5	1.26
90°	2855	47.6	82.8	1.38

The irradiation direction at an angle of 90° had the longest duration of irradiation time and beam-on time, namely 2855 seconds (47.6 minutes) for irradiation time and 82.8 seconds (1.38 minutes) for beam-on time. In contrast, the irradiation direction at an angle of 0° had the shortest duration, with an irradiation time of 2316 seconds (38.6 minutes) and a beam-on time of 71 seconds (1.18 minutes). Meanwhile, the 45° irradiation direction is in between these two angles.

Table 4. Absorptive dose calculation data

Direction of Irradiation	Organ	Dose Threshold Limit (Gy)	Dose in one Fraction (Gy)	Number of fractions	Total Absorbed Dose (Gy)
0°	Skin	2	1.76	34	59.73
	GTV	2	1.99		67.76
	CTV	2	1.99		67.76
	PTV	2	1.99		67.76
	Prostate	2	1.99		67.76
45°	Skin	2	1.66	34	56.33
	GTV	2	1.99		67.80
	CTV	2	1.99		67.80
	PTV	2	1.99		67.80
	Prostate	2	1.99		67.80
90°	Skin	2	2.00	36	71.97
	GTV	2	1.89		67.88
	CTV	2	1.89		67.88
	PTV	2	1.89		67.88
	Prostate	2	1.89		67.88

Based on this calculation, it can be concluded that an increase in the angle of irradiation direction up to 90° results in longer irradiation and beam-on times. This is likely due to changes in dose distribution or target volume coverage, hence requiring longer exposure times.

After obtaining the irradiation time, the absorbed dose can be calculated by equation (3) as presented in Table 4.

Determining the amount of equivalent dose can help assess the potential risk of biological damage caused by radiation exposure. The equivalent dose value can be calculated from equation (4), as in Table 5.

Table 5. Equivalent dose calculation data

Direction of Illumination	Organ	w_R	Equivalent Dose (Gy)
0°	Skin	1	59.73
	GTV	1	67.76
	CTV	1	67.76
	PTV	1	67.76
	Prostate	1	67.76
45°	Skin	1	56.33
	GTV	1	67.80
	CTV	1	67.80
	PTV	1	67.80
	Prostate	1	67.80
90°	Skin	1	71.97
	GTV	1	67.88
	CTV	1	67.88
	PTV	1	67.88
	Prostate	1	67.88

The data presented in Table 5 shows that each irradiation direction (0°, 45°, and 90°) provides variations in the overall absorbed dose to the target organs and their surrounding areas. For the 0° irradiation direction, the skin received a total absorbed dose of 59.73 Gy in 34 fractions with a dose per fraction of 1.76 Gy. Target organs such as GTV, CTV, PTV, and prostate received the same dose of 67.76 Gy with a dose per fraction of 1.99 Gy. The 45° irradiation direction showed a slight decrease in dose to the skin, with a total absorbed dose of 56.33 Gy in 34 fractions. At the same time, other target organs received doses comparable to the dose in the 0° direction. At 90°, the skin received a higher dose (71.97 Gy) in 36 fractions, while the GTV received the highest dose with 67.88 Gy per 2.00 Gy fraction. Other organs, such as the CTV, PTV, and prostate, remained at a dose of 67.88 Gy.

The effective dose rate for skin and prostate were obtained through equation (5), as shown in Table 6.

Table 6. Calculated the effective dose for varied beam directions

Direction of Illumination	Organ	w_T	Effective Dose (Sv)
0°	Skin	0.01	0.61
	Prostate	0.12	8.37
45°	Skin	0.01	0.58
	Prostate	0.12	8.38
90°	Skin	0.01	0.70
	Prostate	0.12	7.92

The data presented shows that the 90° irradiation direction tends to deliver higher doses, especially to the GTV, compared to the 0° and 45° directions. This indicates that the irradiation angle may affect the dose distribution and total absorbed dose in organs, especially the skin and major target organs. Higher doses at larger angles may be necessary to achieve improved coverage of the target volume, though this also leads to increased exposure of normal tissues, including the skin.

In Table 6, the effective dose to the prostate is relatively stable across all irradiation angles. This indicates that increasing the irradiation angle direction affects surface tissues (skin) more than deep target organs, such as the prostate, which receive a consistent effective dose.

The graph shown in Figure 7 shows the relationship between depth (in cm) and total absorbed dose (in Gy) at an irradiation direction of 0 degrees. The highest dose value was recorded at 67.76 Gy at a depth of about 81 cm. After that, the dose tends to decrease gradually until it reaches 21.83 Gy at a depth of 116 cm.

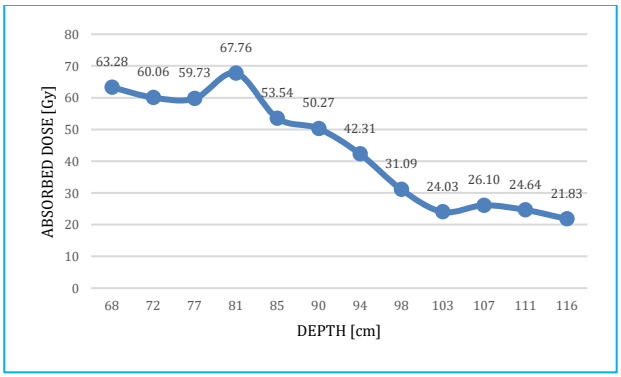

Figure 7. Distribution of Total Absorbed Dose by Depth at 0-Degree Irradiation Direction

The graph in Fig. 8 shows the relationship between depth (cm) and total absorbed dose (Gy) at 45 degrees irradiation direction. The initial dose was 67.05 Gy at a depth of 68 cm and decreased until it reached 46.61 Gy at a depth of 81 cm. After that, there was an increase in dose to the highest peak of 67.80 Gy at a depth of 90 cm, followed by a gradual decrease to 29.10 Gy at a depth of 116 cm.

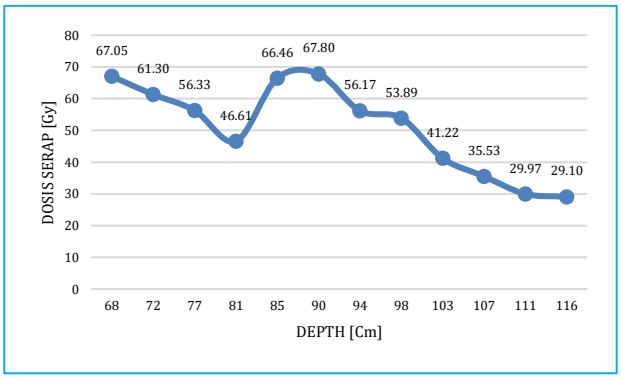

Figure 8. Distribution of Total Absorbed Dose by Depth at 45-Degree Irradiation Direction

The graph in Figure 9 shows the relationship between depth (in cm) and total absorbed dose (in Gy) at 90 degrees irradiation direction. The initial dose was 74.63 Gy at a depth of 68 cm, then increased to the highest peak of 89.20 Gy at a depth of 85 cm. After that, the dose decreased gradually to 35.09 Gy at a depth of 116 cm.

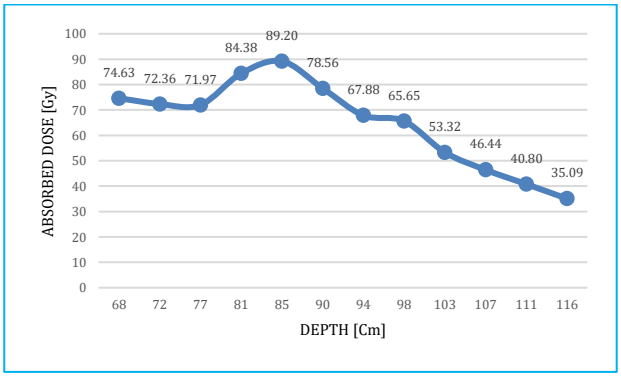

Figure 9. Distribution of Total Absorbed Dose by Depth at 90-Degree Irradiation Direction

An increase in absorbed dose occurs when radiation hits the body surface (skin) within the 77-81 cm depth range, as shown in Fig. 7, Fig. 8, and Fig. 9. This is due to radiation energy that has not been fully absorbed close to the surface. After passing through the surface layer, the absorbed energy increases with depth due to a phenomenon called the build-up effect. The radiation particles generated from the initial interaction continue to interact with the material below the surface, so the absorbed dose increases until it reaches a peak at a certain depth. After reaching the maximum dose, the graph shows a decrease in the absorbed dose. This decrease is due to the attenuation process of radiation as it penetrates the tissue. Radiation loses energy as it is absorbed or scattered by the material it passes through. Hence, the deeper the radiation penetrates the tissue, the less energy remains, and the dose absorbed by the tissue becomes smaller.

Based on the analysis provided, the most effective irradiation angle for prostate cancer

therapy depends on the balance between the effective dose reaching the target (prostate) and minimizing overexposure to healthy tissues such as the skin. At an angle of 0°, the effective dose received by the prostate is quite high. In contrast, the dose received by the skin is relatively low, making it suitable to deliver an effective dose to the prostate without damaging the skin tissue. At an angle of 45°, the effective dose to the prostate remains consistent with the 0° angle, but there is a slight increase in the dose to the skin, although still within safe limits. Using this angle helps expand the tumor volume's coverage without harming the skin. At a 90° angle, although the dose to the prostate remains stable, there is a significant increase in the dose received by the skin. While this angle can provide greater coverage of the target area, care must be taken to avoid causing excessive skin tissue damage.

After considering several important aspects, the optimal irradiation direction is at a 45° angle with a dose of 1.66 Gy per fraction to the skin and 1.99 Gy per fraction to the cancer cells, and a total absorbed dose of 56.33 Gy. This is consistent with Pratama's 2021 research [21], which demonstrated that at 0 degrees, radiation led to complaints of diarrhea due to its effect on the digestive organs. To mitigate these biological impacts, angles of 45 and 90 degrees were employed. The post-irradiation complaints were reduced when these alternative angles were used.

4. CONCLUSION

The most effective irradiation angle for prostate cancer therapy is the 45° angle. At this angle, the effective dose to the prostate remains consistent with the 0° angle, while the dose to the skin experiences a slight increase that is still within safe limits. This allows for expanded coverage of the tumor volume without damaging healthy tissue. While the 0° angle is also effective in delivering a high dose to the prostate with minimal exposure to the skin, the 45° angle offers a balance between treatment effectiveness and lower effective dose to healthy tissue. At the same time, utilizing a 90° angle can considerably raise the dose to the skin while keeping the dose to the prostate consistent, necessitating caution to avoid excessive harm to the skin tissue. With a dose of 1.66 Gy per fraction to the skin and 1.99 Gy per fraction to the cancer cells and a total absorbed dose of 56.33 Gy, a 45° angle is the optimal choice for this therapy.

ACKNOWLEDGMENT

This research would not have been realized without various parties' support, guidance, and valuable contributions. Therefore, we would like to express our gratitude to:

1. The Ministry of Education, Culture, Research, and Technology (KEMENDIKBUD) and the Research Center for Nuclear Safety, Metrology, and Quality Technology of the National Research and Innovation Agency (BRIN) have established the MBKM (*Merdeka Belajar Kampus Merdeka*) internship program.
2. The Ministry of Religious Affairs (KEMENAG) has played an important role in this MBKM program collaboration.
3. UIN Sultan Maulana Hasanuddin Banten provided knowledge, criticism, and suggestions during the completion of this research.

AUTHOR CONTRIBUTION

Tri Nanda Febriansyah: Ideas, formulation or evolution of overarching research goals and aims, development or design of methodology; creation of models, programming, software development, designing computer programs, implementation of the computer PHITS code and supporting algorithms, testing of existing PHITS code components; **Beta Nur Pratiwi:** Verification, whether as a part of the activity or separate, of the overall replication/ reproducibility of results/experiments and other research outputs; **Subur Pramono:** Application of statistical, mathematical, computational, or other formal techniques to analyze or synthesize study data; **Yohannes Sardjono:** Conducting a research and investigation process, specifically performing the experiments, or data/evidence collection; **Gede Sutresna Wijaya:** Provision of study materials, reagents, materials, patients, laboratory samples, animals, instrumentation, computing resources, or other analysis tools; **Isman Mulyadi Triatmoko:** Management activities to annotate (produce metadata), scrub data and maintain research data (including software PHITS code, where it is necessary for interpreting the data itself) for initial use and later reuse; **Nunung Nuraeni:** Preparation, creation and/or presentation of the published work, specifically writing the initial draft (including substantive translation); **Heru Prasetio:** Preparation, creation and/or presentation of the published work, specifically writing the initial draft (including substantive translation); **Nur Rahmah Hidayati:** Preparation, creation and/or presentation of the published work by those from the original research group, specifically critical review, commentary or revision – including pre-or postpublication stages; **Syarifatul Ulya:** Preparation, creation and/or presentation of the

published work, specifically visualization/ data presentation; **Zuhdi Ismail:** Oversight and leadership responsibility for the research activity planning and execution, including mentorship external to the core team cancer therapy.

REFERENCES

1. Bray F., Laversanne M., Sung H., Ferlay J., Siegel R.L., Soerjomataram I., et al. Global Cancer Statistics 2022: GLOBOCAN Estimates of Incidence and Mortality Worldwide for 36 Cancers in 185 Countries. CA. Cancer J. Clin. 2024. 74(3):229–63.
2. ESMO Kanker Prostat: Panduan untuk Pasien. Switzerland: European Society for Medical Oncology; 2022.
3. Ferlay J., Ervik M., Lam F L.M.C.M., Mery L., Piñeros M., Znaor A., et al. Global Cancer Observatory: Cancer Today. 2022 ed. Lyon, France: International Agency for Research on Cancer; 2024.
4. Koka K., Verma A., Dwarakanath B.S., Papineni R.V.L. *Technological Advancements in External Beam Radiation Therapy (EBRT): An Indispensable Tool for Cancer Treatment*. Cancer Management and Research.Dove Medical Press Ltd; 2022.
5. Wang S., Tang W., Luo H., Jin F., Wang Y. *The Role of Image-Guided Radiotherapy in Prostate Cancer: A Systematic Review and Meta-Analysis*. Clinical and Translational Radiation Oncology.Elsevier Ireland Ltd; 2023.
6. Smith S., Prewett S. *Principles of chemotherapy and radiotherapy*. Obstetrics, Gynaecology and Reproductive Medicine.Churchill Livingstone; 2017.
7. Prabhu S., Naveen D.K., Bangera S., Subrahmanya Bhat B. Production of X-RAYS using X-RAY Tube. J. Phys. Conf. Ser. 2020. 1712(1)
8. Park M.Y., Jung S.E. Patient dose management: Focus on practical actions. J. Korean Med. Sci. 2016. 31:S45-54.
9. Nurmansya V.A., Winarno, Miskiyah Z. Radioterapi Kanker Cervix Dengan Linear Accelerator (LINAC). J. Biosains Pascasarj. 2021. 23(02)
10. Fitriatuzzakiyyah N., Sinuraya R.K., Puspitasari I.M. Cancer Therapy with Radiation: The Basic Concept of Radiotherapy and Its Development in Indonesia. Indones. J. Clin. Pharm. 2017. 6(4):311–20.
11. Vaidya J.S. Principles of Cancer Treatment by Radiotherapy. Elseveir. 2024. 42(3):139–49.
12. Jatmiko A.W., Chendra Arum Wandani, Linda Wahyu Istigfarisky Efek Pemakaian Kontras Untuk Optimalisasi Citra Pada Pemeriksaan Diagnostik Magnetic Resonance Imaging (MRI). J. Biosains Pascasarj. 2021. 23(1):28.
13. Elguindi S., Zelefsky M.J., Jiang J., Veeraraghavan H., Deasy J.O., Hunt M.A., et al. Deep Learning-based Auto-segmentation of Targets and Organs-at-risk for Magnetic Resonance Imaging only Planning of Prostate Radiotherapy. Phys. Imaging Radiat. Oncol. 2019. 12:80–6.
14. Li G., Li Y., Wang J., Gao X., Zhong Q., He L., et al. Guidelines for Radiotherapy of Prostate Cancer (2020 edition). Precis. Radiat. Oncol. 2021. 5(3):160–82.
15. Sato T., Iwamoto Y., Hashimoto S., Ogawa T., Furuta T., Abe S.I., et al. Recent Improvements of the Particle and Heavy Ion Transport Code System–PHITS version 3.33. J. Nucl. Sci. Technol. 2024. 61(1):127–35.
16. Kulesza J.A., Adams T.R., Armstrong J.C., Bolding S.R., Brown F.B., Bull J.S., et al. MCNP® Code Version 6.3.0 Theory & User Manual. Code Man. 2022. 28
17. Takada K., Kumada H., Matsumura A., Sakurai H., Sakae T. Computational evaluation of dose distribution for BNCT treatment combined with X-ray therapy or proton beam therapy. Appl. Radiat. Isot. 2020. 165
18. Fuadi N., Jusli N., Harmini Pemantauan Dosis Perorangan Menggunakan Thermoluminescence Dosimeter (TLD) di Wilayah Papua dan Papua Barat Tahun 2020-2021. 2022. 2(1):63–74.
19. Elekta AB *Elekta Versa HD ™*. 2019.
20. Zhang S., Zhang Z.D., Iqbal M., Chi Y.L. Physical Design of A 10 MeV Electron Linac For Industrial Application and Material Irradiation Effect Research. 2022.
21. Pratama M.A.A. *Penatalaksanaan Terapi Radiasi Eksterna Teknik 3D-CRT pada Kasus Kanker Serviks di Instalasi Radioterapi RSUD Arifin Achmad Provinsi Riau*. Pekanbaru:Sekolah Tinggi Ilmu Kesehatan Awal Bros; 2021.
22. Nurhadi I.D., Ramdani R., Haryanto F., Perkasa Y.S., Sanjaya M. Analisis Pengaruh Perubahan Source to Surface Distance (SSD) dan Field Size terhadap Distribusi Dosis Menggunakan Metode Monte Carlo-EGSnrc. Pros. SNIPS. 2016.
23. Luengo D., Martino L., Bugallo M., Elvira V., Särkkä S. *A survey of Monte Carlo Methods for Parameter Estimation*. Eurasip Journal on Advances in Signal Processing.Springer; 2020.
24. Jamal N.H.M., Sayed I.S., Syed W.S. Estimation of Organ Absorbed Dose in

Pediatric Chest X-ray Examination: A Phantom Study. Radiat. Phys. Chem. 2020. 166
25. Urraro F., Nardone V., Reginelli A., Varelli C., Angrisani A., Patanè V., et al. MRI Radiomics in Prostate Cancer: A Reliability Study. Front. Oncol. 2021. 11
26. Zaorsky N.G., Davis B.J., Nguyen P.L., Showalter T.N., Hoskin P.J., Yoshioka Y., et al. *The Evolution of Brachytherapy for Prostate Cancer*. Nature Reviews Urology.Nature Publishing Group; 2017.
27. Gurjar O.P., Arya R., Goyal H. A Study on Prostate Movement and Dosimetric Variation Because of Bladder and Rectum Volume Changes during the Course of Image-guided Radiotherapy in Prostate Cancer. Prostate Int. 2020. 8(2):91–7.
28. Magnetron F.T. Abridged data. 2023. 44(June)
29. T. Sato, Y. Iwamoto, S. Hashimoto, T. Ogawa, T. Furuta, S. Abe, et al. User's Manual PHITS Ver. 3.34. in: *User's Manual PHITS*. English Version ed. 2024.
30. Harish A.F., Warsono, Sardjono Y. Dose Analysis of Boron Neutron Capture Therapy (BNCT) Treatment for Lung Cancer Based on Particle and Heavy Ion Transport Code System (PHITS). ASEAN J. Sci. Technol. Dev. 2020. 35(3):187–94.
31. ICRP Adult Mesh-type Reference Computational Phantoms ANNALS OF THE ICRP PUBLICATION 145. ICRP Publ. 145. 2020. 49(3)

Tri Dasa Mega Vol. xxx No. xxx (year) p1–p2